



ELSEVIER

Available online at www.sciencedirect.com

SCIENCE @ DIRECT®

Nuclear Instruments and Methods in Physics Research B 203 (2003) 130–135

NIM B
Beam Interactions
with Materials & Atomswww.elsevier.com/locate/nimb

Reaction of 5 eV O⁺ with a decanethiolate/Au(1 1 1) self-assembled monolayer

X. Qin, T. Tzvetkov, D.C. Jacobs *

Department of Chemistry and Biochemistry, University of Notre Dame, Notre Dame, IN 46556, USA

Abstract

A beam of 5 eV O⁺ reactively etches a decanethiolate/Au(1 1 1) self-assembled monolayer (SAM). Ion-induced modifications of the SAM are monitored in situ by X-ray photoelectron spectroscopy at different stages during the O⁺ dose. Approximately 3.8 carbon atoms are removed when 10 O⁺ ions strike a decanethiolate molecule; furthermore, 18% of the incident oxygen ions become trapped in the SAM. This facile reactivity is directly compared to that observed for thermal O(³P) incident on an alkanethiolate SAM and to hyperthermal O(³P) bombarding various polymeric films. © 2003 Elsevier Science B.V. All rights reserved.

PACS: 34.50; 61.80; 68.47; 81.15

Keywords: Ion-beam oxidation (IBO); Low-earth orbit (LEO); Hyperthermal O⁺ ion; Ion-beam induced damage; Degradation

1. Introduction

When a hyperthermal ion collides with a surface, the ion's kinetic energy and its electronic potential energy can activate a wide range of chemical reactions [1]. This capacity to induce chemical change is exploited in the fabrication of novel materials and coatings; on the other hand, the heightened reactivity of ions can be deleterious to spacecraft exposed to the low-earth orbit (LEO) environment [2]. The most abundant ion in LEO is O⁺; within the rest frame of an orbiting space vehicle at 300 km altitude, ambient O⁺ will strike the surface of the spacecraft with a collision energy of ~5 eV [3]. The damage caused by materials

degradation and erosion in LEO can shorten the lifespan and viability of a space mission. Consequently, great efforts are expended on identifying new materials and coatings that are resistant to LEO attack [4]. Polymeric materials are attractive candidates, because they are lightweight, inexpensive, and moldable. As a preliminary test of their viability for spacecraft applications, a series of satellite-based measurements have determined the erosion rates for simple polymers (e.g. polyethylene, kapton and teflon) in LEO [5]. However, laboratory-based simulations of the LEO environment have failed to achieve as high of an etch rate using neutral O-atom sources [6]. Potential synergistic effects involving electron-, photon-, and ion-bombardment may accelerate the reactivity of O-atoms in LEO [7].

To gather mechanistic information about the interaction of O⁺ with saturated hydrocarbon

* Corresponding author.

E-mail address: jacobs.2@nd.edu (D.C. Jacobs).

polymers, experiments must be performed on well-characterized surfaces. One model surface that serves as a prototype for polyethylene is an alkanethiolate self-assembled monolayer (SAM) [8]. Alkanethiol molecules bind tightly to gold through the sulfur group. On crystalline Au(111), decanethiol forms close-packed ordered domains of parallel hydrocarbon chains, tilted at 34° relative to the surface normal [9]. These surfaces represent stable, well-characterized interfaces for studying the reactivity of ions with saturated hydrocarbons [10–12]. Because the monolayer is only 14.5 Å thick, there is not significant charging by the incident ion beam during the experiment.

Fairbrother and coworkers have studied the reaction of thermal O/O₂ with a decanethiolate SAM [13]. The oxygen atoms were generated in a thermal gas cracker and effused through a small aperture to strike the surface. The researchers employed X-ray photoelectron spectroscopy (XPS) to monitor the chemical composition of the SAM as a function of oxygen dose. In addition to observing a significant decrease in the surface carbon signal, they saw evidence for extensive oxidation of the hydrocarbon chain. The authors surmised that carbon is removed via the desorption of volatile oxidation products, such as CO(g) or CO₂(g), formed through hydrogen abstraction followed by oxygen addition.

George and coworkers investigated the degradation of an octadecanethiolate SAM exposed to an oxygen plasma [14]. They compared the etch rate for the complete plasma (neutrals, ions, and electrons) to the etch rate measured for the neutral plasma species alone. The presence of charged particles in the incident flux enhanced the etch rate by approximately a factor of five. It is unclear, however, whether the increased impact energy or an increased chemical reactivity is responsible for the ions' added reactivity. Koontz et al. presented a critical review of polymer-degradation experiments involving thermal (<0.1 eV) versus hyperthermal (3 eV) neutral O-atom sources [6]. For all organic surfaces studied, hyperthermal O-atom sources better emulate the polymer-erosion measurements collected in the LEO environment.

In the present study, the reaction of 5 eV O⁺ with a decanethiolate SAM is studied under ul-

trahigh vacuum (UHV) conditions. In situ XPS reveals the rate at which the hydrocarbon layer is oxidized and etched by the incident ion beam. Comparison is made to similar experiments involving predominantly neutral oxygen reactants.

2. Experimental

The experiments are conducted in an UHV scattering chamber described elsewhere [15,16]. A Au(111) crystal is Ar-sputtered (300 eV) and annealed at 550 °C in UHV to prepare an atomically clean, well-ordered surface, as verified by XPS and low-energy electron diffraction. The crystal is removed through a vacuum load-lock and submerged for 24 h in 1 mM decanethiol/ethanolic solution. After the sample is removed from the solution, it is rinsed in pure ethanol and dried with blown nitrogen. Quickly, the substrate is reloaded into the UHV chamber and left under vacuum for 18–24 h at room temperature to remove any excess solvent.

The reactant oxygen ions are generated in a Colutron plasma source, accelerated to 1.5 keV, mass-selected in a Wien filter, and decelerated to the final beam energy of 5.0 eV (2.4 eV FWHM). The ion beam is directed at normal incidence to the surface with a current density equal to 50–60 nA/cm². Periodically, the oxygen dose is interrupted, and the surface is positioned in front of an XPS spectrometer, mounted within the same chamber. After XPS spectra of the Au 4f, C 1s, and O 1s peaks are collected, the sample is repositioned for further oxygen dosing. All experiments are conducted at room temperature.

The XPS measurements utilize a Mg K α X-ray source operated at 260 W (13 kV) and a VG 100AX hemispherical analyzer. Spectral analyses consisted of background subtraction followed by peak fitting. A Tougaard background is subtracted from the C 1s peak, whereas linear backgrounds are subtracted from both the Au 4f and O 1s peaks. The C 1s spectra are fit with 1–3 peaks (85% Gaussian/15% Lorentzian peak shapes) centered on the unoxidized C(0) and oxidized C(I) or C(II) peak positions. The carbon peaks are constrained to share a common, fixed FWHM.

3. Results and discussion

Fig. 1 shows the C 1s region of XPS spectra recorded before and after the SAM was exposed to 4.5×10^{15} O⁺ ions/cm². A third spectra in Fig. 1 corresponds to a control run, in which the experimental procedure described above is repeated, except that the ion beam is deflected from the surface. Although the control run demonstrates that X-ray irradiation, by itself, leads to a partial depletion of carbon in the film, the O⁺ dose significantly accelerates the process. In addition, it is apparent that after O⁺-bombardment the SAM layer exhibits a small shoulder to high binding energy in the C 1s XPS spectrum. The shoulder is

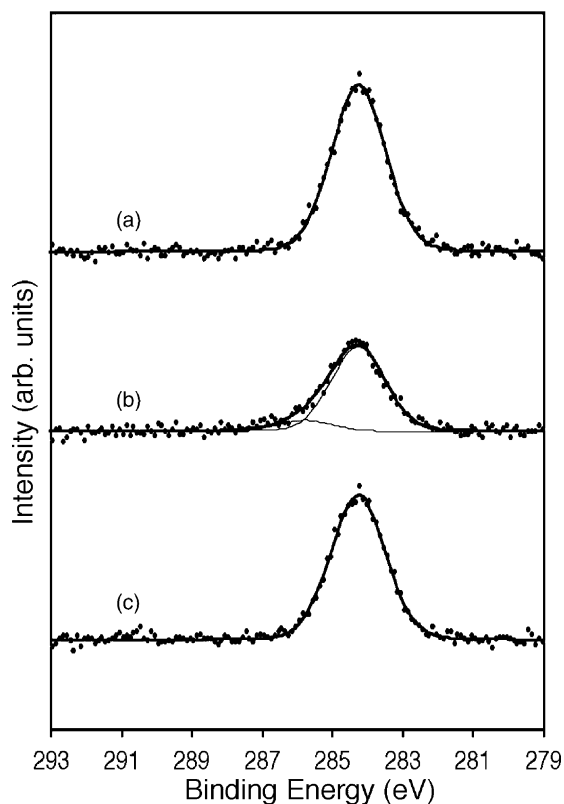


Fig. 1. C(1s) region of XPS spectra for decanethiolate SAM on Au(111). The spectra are recorded (a) initially, (b) after an O⁺ exposure of 4.5×10^{15} ions/cm² and (c) following a control run in which the O⁺ ion beam was deflected from the surface. Spectrum (b) is fit to contributions from two oxidation states: C(0) and C(I).

assigned to oxidized C(I) in the form of $\begin{array}{c} | \\ -\text{C}-\text{O}-\text{H} \\ | \end{array}$ or $\begin{array}{c} | \\ -\text{C}-\text{O}-\text{C}- \\ | \end{array}$ functional groups. There is no discernable oxidation in the control run.

In tandem with each C 1s spectrum, Au 4f and O 1s spectra are recorded. Commensurate with the depletion in the C 1s signal, the area under the Au 4f peak increases slightly with O⁺ dose, consistent with a systematic thinning of the carbon layer through ion etching. Taking into account the X-ray cross-sections and inelastic mean free paths of photoelectrons ejected from Au and C, the carbon-layer thickness is calculated for each O⁺ dose [17]. Fig. 2 presents the thickness of the carbon layer, and correspondingly the number of carbon atoms per decanethiolate molecule, as a function of O⁺ exposure. The data collected from the control experiment are overlaid on the same plot. Although X-rays alone appear to damage the

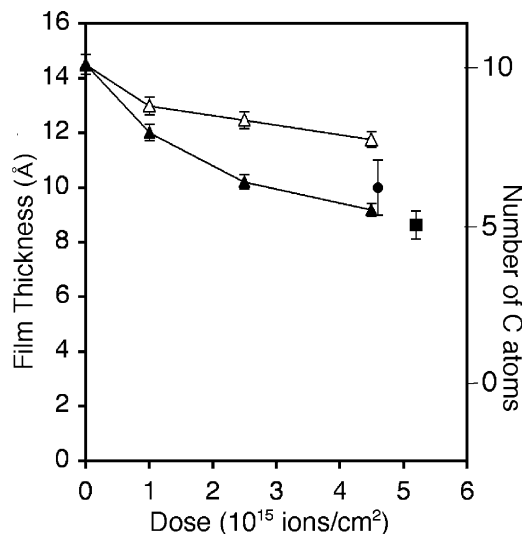


Fig. 2. Thickness of SAM layer, and the corresponding number of carbon atoms per hydrocarbon chain, as a function of O⁺ dose. The solid triangles represent the data collected with the O⁺-beam on. The open triangles arise from the control experiment, in which the same procedure was followed with the O⁺-beam off. The solid circle results when only one set of X-ray spectra is recorded before O⁺ exposure, and no X-rays were delivered during the O⁺ dose. Similarly, the solid square indicates the result when no X-ray irradiation was employed until after the entire O⁺ dose.

film, the SAM treated with 5 eV O^+ is etched more severely.

The X-ray induced damage to SAMs on Au is well-documented and leads to hydrogen and carbon loss as well as interchain linking [18,19]. Although the X-ray source did not alter the surface temperature, low-energy electrons emitted from the source could contribute to the degradation of the SAM. To address the potential interference that X-ray damage may impose upon the ion etching results, experiments are repeated in which the sequence and magnitude of O^+ and X-ray doses are varied widely. For example, rather than record periodic XPS spectra during the O^+ dose (see solid triangles in Fig. 2), a run is performed in which XPS spectra are taken only at the beginning and end of the run (see solid square in Fig. 2). Although the latter experiment has a lower X-ray dose during the oxidation step, albeit a comparable overall X-ray dose, the two runs result in a similar loss of carbon. To eliminate all pretreatment of the SAM with X-rays, a run is performed in which the first XPS is not recorded until after the entire O^+ dose is finished.¹ Within a few minutes after commencing X-ray exposure, the C and Au spectra are completely recorded (resulting in the solid circle in Fig. 2). This latter point provides a reasonably accurate assessment of the ion-induced damage with minimal X-ray induced modifications. Taking into account various scenarios for the confluence of 5 eV O^+ and X-ray bombardment in all of the data sets recorded, we conclude that, on average, 3.8 ± 0.7 carbon atoms are removed for every ten 5 eV O^+ ions impacting a decanethiolate molecule.

The 5 eV ion energy is insufficient to physically sputter an entire decanethiolate molecule intact. Furthermore, an O^+ ion strikes each decanethiolate molecule once every 20 min; hence, the infrequency of collisions prevents collective physical sputtering effects. Auger neutralization of O^+ could degrade the SAM through potential hot-electron emission; however, this is unlikely because

¹ The SAM deposition process resulted in highly reproducible XPS spectra in which the C/Au peak areas on separate samples differed by only a few percent.

the ionization potential (13.6 eV) of oxygen is less than twice the energy gap (7.4 eV) between the highest occupied and lowest unoccupied levels of the saturated hydrocarbon layer [20]. Instead, the carbon atoms are stripped from the decanethiolate molecules sequentially. Previous authors have conjectured that oxidation of the hydrocarbon chain precedes and initiates carbon removal [6,13]. Indeed, the shoulder feature in the C 1s XPS spectra (Fig. 1(b)) develops with O^+ exposure. Fig. 3 plots the ratio of the area under the carbon shoulder peak(s), divided by the area under the entire carbon peak, as a function of the O^+ dose. Further evidence for the incorporation of oxygen into the SAM appears in the O 1s XPS spectrum. Fig. 3 shows the area under the O 1s peak, scaled

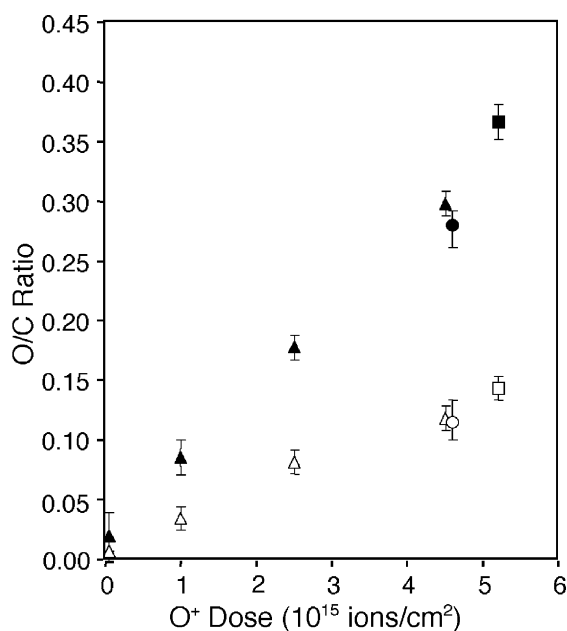


Fig. 3. Oxygen-to-carbon ratio in the film as a function of O^+ dose. The total oxygen-to-carbon ratio (solid symbols) is derived from comparing the peak areas under the O 1s and C 1s XPS spectra. The open symbols represent the subset of oxygen bound to carbon scaled by the total amount of carbon, as calculated from the peak areas within a C 1s spectrum. Triangles designate XPS data recorded at periodic intervals during the O^+ exposure. Squares symbolize data collected when only one set of X-ray spectra is recorded before O^+ exposure, and no X-rays were delivered during the O^+ dose. Circles indicate the analogous result when no X-ray irradiation was employed until after the entire O^+ dose.

Table 1
Recession rates for polymeric materials (per incident oxygen nucleus)

Projectile	Energy (eV)	Polymeric material	Recession rate (cm ³ /atom)
O ⁺	5	CH ₃ (CH ₂) ₉ S/Au SAM	(7.5–11.7) × 10 ⁻²⁴ (this work)
O	<0.1	CH ₃ (CH ₂) ₁₅ S/Au SAM	7.4 × 10 ⁻²⁸ [13]
O	<0.1	CH ₃ (CH ₂) ₁₇ S/Au SAM	2.6 × 10 ⁻²⁶ [14]
O	<0.1	Polyethylene	(0.9–4.0) × 10 ⁻²⁷ [6]
O	3	Polyethylene	2.8 × 10 ⁻²⁴ [6]
LEO O, O ⁺ , e ⁻ , hν	5	Polyethylene	3.7 × 10 ⁻²⁴ [6]
O	<0.1	Kapton (polyimide)	(1.2–5.4) × 10 ⁻²⁸ [6]
O	3	Kapton (polyimide)	2.7 × 10 ⁻²⁴ [6]
LEO O, O ⁺ , e ⁻ , hν	5	Kapton (polyimide)	3.0 × 10 ⁻²⁴ [6]

to that for the C 1s peak, while correcting for their respective sensitivity factors. This provides an upper limit on the oxygen content in the SAM, because it is likely that the mean depth of carbon in the film is greater than the mean depth of oxygen; hence, the oxygen signal will be attenuated less than the carbon signal. Prolonged exposure to X-rays had no effect on the O/C ratio measured. However, X-ray exposure did reduce the ratio of the oxidized to nonoxidized carbon components by 15–20%. The control experiment, described at the beginning of this section, resulted in no detectable levels of oxygen in the SAM.

The two independent measures of oxygen content in the SAM, indicated by solid and open symbols in Fig. 3, differ by a factor of two. Whereas the O/C ratio is sensitive to all forms of oxygen, the proportion of oxidized to total carbon in the SAM provides information about only the subset of oxygen atoms that are bound to carbon. The data suggest that ~60% of the oxygen incorporated in the film may be in the form of H₂O or O₂. Temperature-programmed desorption spectra, recorded at the end of the O⁺ dose, show no evidence for H₂, O₂, CO, or CO₂ emission. However, there is a considerable H₂O desorption peak, suggestive that water is a major byproduct of ion-beam oxidation. More experiments are necessary to rule out adventitious sources of water in the TPD spectra. In summary, the data indicate that after a dose of 10 O⁺ ions per decanethiolate molecule, an average of 3.8 ± 0.7 carbon atoms are lost, 0.7 ± 0.1 oxygen atoms are incorporated into each alkane chain, and 1.1 ± 0.2 oxygen atoms are trapped in the SAM – potentially in the form of water.

The efficiency with which 5 eV O⁺ etches a decanethiolate SAM layer can be directly compared to laboratory and space-based experiments on similar systems. Table 1 lists the recession rates (i.e. volume of material removed by an incident particle) measured for thermal and hyperthermal, neutral O-atoms incident on hydrocarbon SAMs, polyethylene, and kapton films. In comparing our results to thermal O-atom studies on comparable alkanethiolate SAMs, it is apparent that 5 eV O⁺ ions etch an alkanethiolate SAM with two to four orders of magnitude greater efficiency than do 0.1 eV O-atoms. The hydrocarbon density within the decanethiolate SAM is close to that of polyethylene, a saturated hydrocarbon polymer. The similarity of these two surfaces is supported by the fact that thermal O-atom erosion studies on polyethylene are bracketed by the results for the alkanethiolate SAM analogs [6,13,14]. If comparison is made between the results for 5 eV O⁺/SAM and 3 eV O/polyethylene systems, the ions appear to be more reactive. In fact, the recession rate measured in the present study exceeds that recorded for polyethylene or kapton in LEO, where neutrals, ions, electrons, and photons act synergistically. Although ions are a minority species in LEO, they may induce a disproportionate share of the damage inflicted upon spacecraft materials.

Acknowledgements

This work was conducted at the University of Notre Dame through the Center for Materials Chemistry in the Space Environment, a

Multidisciplinary University Research Initiative (MURI) supported by the Air Force Office of Scientific Research.

References

- [1] D.C. Jacobs, *Ann. Rev. Phys. Chem.* 53 (2002) 379.
- [2] D.C. Jacobs, in: R. Dressler (Ed.), *Chemical Dynamics in Extreme Environments*, World Scientific Publishers, 2000.
- [3] E. Murad, *Ann. Rev. Phys. Chem.* 49 (1998) 73.
- [4] M.R. Reddy, *J. Mater. Sci.* 30 (1995) 281.
- [5] M.C. Lillis, E.E. Youngstrom, L.M. Marx, A.M. Hammerstrom, K.D. Finefrock, C.A. Youngstrom, C. Kaminiski, E.S. Fine, P.K. Hunt, K.K. de Groh, B.A. Banks, E.A. Sechkar, NASA TM-2002-211553 (2002).
- [6] S.L. Koontz, K. Albyn, L.J. Leger, *J. Spacecraft Rockets* 28 (1991) 315.
- [7] J.I. Kleiman, Z.A. Iskanderova, F.J. Pérez, R.C. Tennyson, *Surf. Coat. Technol.* 76 (1995) 827.
- [8] F.M. Elms, G.A. George, *Polym. Adv. Technol.* 9 (1998) 31.
- [9] N. Camillone III, P. Eisenberger, T.Y.B. Leung, P. Schwartz, G. Scoles, G.E. Poirier, M.J. Tarlov, *J. Chem. Phys.* 101 (1994) 11031.
- [10] J.A. Burroughs, L. Hanley, *Anal. Chem.* 66 (1994) 3644.
- [11] J. Shen, Y.H. Yim, B. Feng, V. Grill, C. Evans, R.G. Cooks, *Int. J. Mass Spectrom.* 182/183 (1999) 423.
- [12] V.J. Angelico, S.A. Mitchell, V.H. Wysocki, *Anal. Chem.* 72 (2000) 2603.
- [13] J. Torres, C.C. Perry, S.J. Bransfield, D.H. Fairbrother, *J. Phys. Chem. B* 106 (2002) 6265.
- [14] X.J. Dai, F.M. Elms, G.A. George, *J. Appl. Polym. Sci.* 80 (2001) 1461.
- [15] C.L. Quinteros, T. Tzvetkov, X. Qin, D.C. Jacobs, *Nucl. Instr. and Meth. B* 182 (2001) 187.
- [16] T. Tzvetkov, X. Qin, D.C. Jacobs, *Phys. Rev. B*, in press.
- [17] L.T. Weng, G. Vereecke, M.J. Genet, P. Bertrand, W.E.E. Stone, *Surf. Interface Anal.* 20 (1993) 179; L.T. Weng, G. Vereecke, M.J. Genet, P.G. Rouxhet, J.H. Stone-Masui, P. Bertrand, W.E.E. Stone, *Surf. Interface Anal.* 20 (1993) 193.
- [18] B. Jäger, H. Schürmann, H.U. Müller, H.-J. Himmel, M. Neumann, M. Grunze, Ch. Wöll, *Z. Phys. Chem.* 202 (1997) 263.
- [19] M. Wirde, U. Gelius, T. Dunbar, D.L. Allara, *Nucl. Instr. and Meth. B* 131 (1997) 245.
- [20] B.L. Sowers, M.W. Williams, R.N. Hamm, E.T. Arakawa, *J. Chem. Phys.* 57 (1972) 167.